Available online at www.sciencedirect.com
SCIENCE @ DIRECT®

Polymer 45 (2004) 1297–1306

polymer
www.elsevier.com/locate/polymer

Substituted poly(silylenemethylene)s with short range interactions that induce a preference for the same local conformation in unperturbed atactic, isotactic, and syndiotactic chains

Carin A. Helfer[a], Wayne L. Mattice[a,*], Donghai Chen[b]

[a]*Institute of Polymer Science, The University of Akron, Akron, OH 44325-3909, USA*
[b]*Department of Natural Science, Malone College, Canton, OH 44709, USA*

Received 13 November 2002; received in revised form 11 March 2003; accepted 15 March 2003

Abstract

A rotational isomeric state model has been developed for the poly(silylenemethylenes) with repeating sequence $[Si(CH_3)R{-}CH_2]_x$, $R = -O(CH_2)_NOC_6H_4C_6H_5$. The model incorporates all first- and second-order interactions, as well as higher order interactions that are mandatory in some of the conformations. Chains with all possible stereochemical sequences prefer a local conformation that is a run of *trans* states at the C–Si bonds in the backbone. This preference arises from an attractive second-order interaction of the first methylene group in the side-chain bonded to chain atom *i* with the silicon atoms indexed $i \pm 2$. Unperturbed chains have larger dimensions than the simpler chain in which R is merely a methyl group. The temperature coefficients of the unperturbed dimensions are large and negative. The preference of unperturbed atactic, isotactic, and syndiotactic chains for the same local conformation may contribute to the facile formation of smectic phases by the presumably atactic chain, as reported by Park et al. [Macromolecules 35 (2002) 2776].

Keywords: Conformation; Poly(silylenemethylene); RIS

---

1. Introduction

Polymers with the repeating sequence $XRR'{-}CH_2$ usually have physical properties that depend on the stereochemical sequence [1–3]. Polypropylene ($X = C$, $R = CH_3$, $R' = H$) and polystyrene ($X = C$, $R = C_6H_5$, $R' = H$) are common examples. At sufficiently low temperature, a chain with a repeating sequence of dyads crystallizes as a helix with two [4,5] or more [1–3] units per turn. In contrast, the atactic chain resists the adoption of a regular helical structure at low temperature, and instead becomes an amorphous glass upon cooling.

This expectation for the atactic chain can sometimes be overcome when R contains a bulky group. The bulky side-chains may pack in specific helical conformations, with 2–7 monomer units per turn, even when the conditions of the synthesis are expected to lead to an atactic polymer. Examples are provided by poly(methacrylates) with dendritic side groups [6] and poly(silylenemethylenes) with side-chains that terminate in biphenyl units [7]. These interesting observations raise several questions. Does the periodic arrangement of the bulky side-chains require an ordered conformation of the atactic backbone? If so, how do the short-range intramolecular interactions permit the formation of a regular periodic structure by the atactic main chain? Would modification of the stereochemical sequence alter the stability of the ordered structure, or perhaps lead to the formation of a different ordered structure?

One approach to these questions is to inquire when short-range intramolecular interactions might induce a preference for a regular periodic structure in an atactic chain. Here we use a rotational isomeric state (RIS) analysis to identify one such short-range interaction in the substituted poly(silylenemethylenes). Specifically, we consider $[Si(CH_3)R{-}CH_2]_x$, where R is a flexible spacer terminated with a biphenyl unit, $-O(CH_2)_NOC_6H_4C_6H_5$ [7]. The model incorporates all first- and second-order interactions, as well as the higher order interactions that are mandatory in some of the conformations. Illustrative calculations are presented at 373 K, which is

---

* Corresponding author. Tel.: +1-330-972-5128; fax: +1-2330-972-5396.
E-mail address: wlm@polymer.uakron.edu (W.L. Mattice).

0032-3861/$ - see front matter © 2003 Elsevier Ltd. All rights reserved.
doi:10.1016/j.polymer.2003.03.004

slightly above the temperature (356–367 K) of the smectic → isotropic transition of the substituted poly(silylenemethylene)s with $N = 3$, 6, 8, and 11 [7].

Simulation of the facile formation of smectic phases by the poly(silylenemethylenes) below 356–367 K should employ atomistically detailed multi-chain models of the polymers at bulk density. In practice, however, the time required for equilibration of the dense multi-chain models, with bulky aromatic side-chains appended to alternate atoms in the main chain, requires computational resources that are not currently available. Equilibrated models require an alternative approach, which provides a second motivation for the development of an RIS model for these polymers.

A coarse-grained model of a dense polymer system can be equilibrated more easily than the atomistically detailed representation of the same system [8]. Constraints can be imposed on a coarse-grained model that permit ‘reverse-mapping’ to an atomistically detailed model [9]. These constrained coarse-grained models can accurately reproduce subtle aspects of the real systems they represent, as illustrated by applications to polypropylene melts [10]. Simulations with constrained coarse-grained chains reproduce the experimental observations for melts that atactic and isotactic polypropylene are miscible [11,12], but syndiotactic polypropylene demixes from either atactic or isotactic polypropylene [12–14]. The simulation identifies the molecular mechanism responsible for this behavior [10,15,16].

Two distinctly different constraints are imposed on the coarse-grained chains in these simulations. A short-range intramolecular constraint, imposed via the mapping of a RIS model [17], insures the proper distribution for the end-to-end vector for the entire chain, as well as the end-to-end vector for all of its subchains [18,19]. Intermolecular interactions, and long-range intramolecular interactions, are handled by a discretized version of a continuous potential energy function [20]. The constraints in the simulation of the coarse-grained models of melts of polypropylene were constructed from a RIS model for this polymer and the Lennard–Jones potential energy function that describes the interaction of pairs of molecules of propane [10]. The phenyl group of polystyrene is the largest side-chain present in previous applications of this type of simulation [21]. So far there has been no attempt to use this method for the simulation of side-chain liquid crystalline polymers. The second motivation for the development of the RIS model for the substituted poly(silylenemethylenes) is in anticipation of application of this type of simulation to the formation of smectic phases by these polymers [7].

2. Polymers with repeating sequences $SiH_2–CH_2$ or $Si(CH_3)_2–CH_2$

Although our primary interest here is in the poly(silylenemethylenes) for which highly ordered smectic phases have been reported by Interrante, Farmer, and co-workers, it is useful to begin the study with a consideration of the relevant properties of the RIS models for two simpler polymers with the repeating sequences $–SiH_2–CH_2–$ and $–Si(CH_3)_2–CH_2–$. Stereochemical composition is not an issue in these two simpler chains.

The general form of the statistical weight matrix for bond i in a chain with pair-wise interdependent bonds subject to a symmetric three-fold torsion potential is given by Eq. (1) [17].

$$\mathbf{U}_i = \begin{bmatrix} \tau & \sigma & \sigma \\ 1 & \sigma\psi & \sigma\omega \\ 1 & \sigma\omega & \sigma\psi \end{bmatrix}_i \tag{1}$$

Rows (or columns) are indexed by the state at bond $i-1$ (or i) in the order *trans* (t), *gauche* + ($g+$), *gauche* − ($g-$). The first-order statistical weight of either g state relative to t is denoted by σ. The second-order statistical weights are assigned using tg ($= gt$) as a reference, with τ being the statistical weight for the tt sequence, while ψ (or ω) are statistical weights for two consecutive g states of the same (or opposite) sign. The conformational partition function, Z, for a chain with n bonds is obtained as the serial product of n statistical weight matrices.

$$Z = \mathbf{U}_1\mathbf{U}_2 \ldots \mathbf{U}_n \tag{2}$$

The terminal matrices are the special cases $\mathbf{U}_1 = [1 \quad 0 \quad 0]$ and $\mathbf{U}_n = [1 \quad 1 \quad 1]^T$ [17].

Estimates of the energies of the first- and second-order interactions for poly(silaethylene), $(SiH_2–CH_2)_x$, were derived from conformational energy calculations (using the Universal 1.02 force field and Cerius^2 version 4.0 from Accelrys, Inc.) for $SiH_3–CH_2–SiH_2–CH_3$, $CH_3–SiH_2–CH_2–SiH_2–CH_3$, and $SiH_3–CH_2–SiH_2–CH_2–SiH_3$. When compared with the corresponding n-alkanes, the short-range interactions are weakened by replacement of the shorter (1.54 Å) C–C bonds by longer (1.89 Å) C–Si bonds. Analysis of these conformational energy surfaces leads to estimates of first- and second-order interactions energies that are collected in the first two rows of Table 1. Abe et al. deduced stronger interactions, $E_\sigma = 2$ kJ/mol and $E_\omega = 8$ kJ/mol, for polyethylene (PE) [22]. Recent ab initio calculations for $SiH_3–CH_2–SiH_2–CH_3$ and $SiH_3–CH_2–SiH_2–CH_2–SiH_3$ suggest $E_\sigma = 0.9$ kJ/mol, as well as $E_\tau = 0$, $E_\psi = -0.6$, and $E_\omega = 4.2$ kJ/mol for the Si–C bond [23].

Table 1
First- and second-order interaction energies (kJ/mol) in poly($SiR_2–CH_2$), R = H or CH_3. The results for the latter polymer are from Mark and Ko [24]

R	Bond i	E_σ	E_τ	E_ψ	E_ω
H	C–Si	0.7	0.1	0.3	3.0
H	Si–C	0.7	0.5	−0.4	4.6
CH_3	C–Si	0	0	0	0.8
CH_3	Si–C	0	0	0	∞

These ab initio results are within a few tenths of a kJ/mol of the energies cited in Table 1. In the hands of these authors, the most stable conformation for the C–Si bond shifted from *t* to *g* when the ab initio calculations were replaced by a semi-empirical method (Spartan, Version 4). The present calculations using Universal 1.02 force field and Cerius^2 version 4.0 are in better agreement with the ab initio results of Park et al. than are their semi-empirical results, because $E_\sigma > 0$ implies that the *t* state is preferred at the C–Si bond.

Table 2 will track the changes in the mean square unperturbed dimensions and the occupancy of the *t* state as the RIS model is changed step by step from PE to $(\mathrm{SiCH_3R{-}CH_2})_x$, $\mathrm{R = O(CH_2)_{\mathit{N}}OC_6H_4C_6H_5}$. The data are tabulated at 373 K, which is slightly above the temperature (356–367 K) of the smectic → isotropic transition of the substituted poly(silylenemethylenes) with $N = 3$, 6, 8, and 11 [7].

The fraction of the bonds in the three states, p_η, is extracted from Z with the customary partial derivative of Z [17].

$$p_{g^+} = p_{g-} = \frac{1-p_t}{2} = \frac{1}{2(n-2)}\left(\frac{\partial \ln Z}{\partial \ln \sigma}\right) \tag{3}$$

At 373 K, the interaction energies in the first two rows of Table 1 specify $p_t = 0.47$, which is smaller than the value of 0.60 obtained from the RIS model for unperturbed PE at the same temperature. The silicon-containing polymer prefers the *t* state, but that preference is not as strong as it was in PE. Poly(silaethylene) crystallizes in a planar zigzag conformation [25], which is consistent with the *t* state being preferred in the unperturbed chain. The melting temperature of about −20 °C is much lower than T_M for PE, which is consistent with a smaller preference for *t* states in poly(silaethylene) than in PE.

The characteristic ratio, $C = \langle r^2\rangle_0/nl^2$, of the mean square unperturbed end-to-end distance, $\langle r^2\rangle_0$, is calculated from Z, the bond length, l, the bond angle, θ, and the torsion angles, ϕ [17]. At 373 K, $C_\infty = 4.2$ and $\mathrm{d}\ln\langle r^2\rangle_0/\mathrm{d}T = -1.1\times10^{-3}\ \mathrm{K}^{-1}$. This C_∞ is only 2/3 of the value from the RIS model for unperturbed PE, as expected from the smaller value of p_t. The temperature coefficient, however, is similar to the value found in PE [22].

A simpler set of statistical weights, listed in the last two lines of Table 1, was adopted by Mark and Ko for poly(dimethylsilylenemethylene) with a repeating sequence of $[\mathrm{Si(CH_3)_2{-}CH_2}]_x$ [24]. An even simpler model, with $E_\omega = 0$ in the statistical weight matrix for the C–Si bond, was used by Sundararajan [26]. The simplification upon changing the repeating unit from $\mathrm{SiH_2{-}CH_2}$ to $\mathrm{Si(CH_3)_2{-}CH_2}$ arises from the equivalence of the first-order interactions in all of the states in the latter polymer, in the approximation that methylene and methyl groups participate in similar interactions, as shown in Fig. 1. The second-order interaction of two bulky $\mathrm{Si(CH_3)_2}$ groups in the $g+g-$ and $g-g+$ states is so severe that it can be taken to be infinite. These conformations produce mandatory third-order interactions of one Si atom with a carbon atom bonded to the other Si atom, with the interaction distance being the same as the Si–C bond length. Carbon atoms bonded to these two silicon atoms overlap prohibitively, as shown in Fig. 2. The RIS model of Mark and Ko specifies $p_\mathrm{t} = 0.44$ at 373 K. The polymer comes closer to having equivalent populations in all three states than does poly(silaethylene) because the first-order interaction is vanishingly small, $\sigma = 1$. The slight excess of *t* states arises from the penalty applied to pairs of successive *g* states of opposite sign, $\omega < 1$. Since p_t is closer to the prediction for equal population of all three states, the characteristic ratio becomes slightly smaller, $C_\infty = 3.7$ at 373 K, and its temperature coefficient is closer to zero, $\mathrm{d}\ln\langle r^2\rangle_0/\mathrm{d}T = -0.19\times10^{-3}\ \mathrm{K}^{-1}$. This simple model provides reasonable agreement with the experimental temperature coefficient, which is very close to zero, $(0.21\pm0.15)\times10^{-3}\ \mathrm{K}^{-1}$, but the agreement with the experimental characteristic ratio, $C = 5.32\pm0.01$, is less satisfactory [27]. Part of the discrepancy in the calculated and experimental values of C has been attributed to the likelihood that the Si–C–Si bond angle is larger than tetrahedral in this polymer [24].

Lengthening of the side-chains may alter the preferred

Table 2
Occupancy of the *t* state and mean square dimensions for several RIS models at 373 K, using tetrahedral bond angles and torsion angles of 180° and ±60°

Repeat unit	p_t	p_{tt}	C_∞
$\mathrm{CH_2{-}CH_2}$[a]	0.60	0.33	6.38
$\mathrm{SiH_2{-}CH_2}$	0.47	0.19	4.15
$\mathrm{Si(CH_3)_2{-}CH_2}$[b]	0.44	0.17	3.67
$\mathrm{Si(CH_3)R{-}CH_2}$, R = O, $p_\mathrm{m} = 0$[c]	0.55	0.29	4.66
$\mathrm{Si(CH_3)R{-}CH_2}$, R = O, $p_\mathrm{m} = 1$[c]	0.52	0.22	4.48
$\mathrm{Si(CH_3)R{-}CH_2}$, $\mathrm{R = O(CH_2)_3OC_6H_4{-}C_6H_5}$, $p_\mathrm{m} = 0$	0.76	0.60	9.96
$\mathrm{Si(CH_3)R{-}CH_2}$, $\mathrm{R = O(CH_2)_3OC_6H_4{-}C_6H_5}$, $p_\mathrm{m} = 1$	0.69	0.47	7.09

[a] Using $E_\sigma = 2$ kJ/mol and $E_\omega = 8$ kJ/mol [22].

[b] Using the model of Mark and Ko [24].

[c] Hypothetical polymer in which R is truncated to a single oxygen atom.

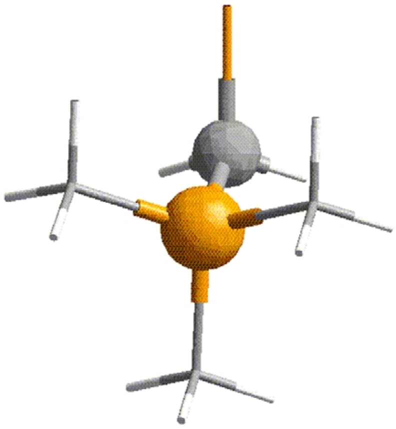

Fig. 1. Newman projection along the internal Si–C bond (with these two atoms represented by spheres) in $\mathrm{Si(CH_3)_3{-}CH_2{-}Si}$.

Fig. 2. Mandatory and prohibitively repulsive higher-order interactions when there are g states of opposite sign at the two bonds to the central silicon atom in $(CH_3)_3Si{-}CH_2{-}Si(CH_3)_2{-}CH_2{-}Si(CH_3)_3$.

conformation of the backbone of $(SiR_2{-}CH_2)_x$, as shown by comparison of the polymers with methyl and *n*-propyl side-chains. Fibers drawn from the isotropic melt of poly(di-*n*-propylsilylenemethylene) at 80 °C are crystalline at room temperature [23]. The *c*-axis of 4.86 Å has been interpreted as arising from a 4_1 helix in which the C–Si bonds in the backbone adopt g placements of the same sign. This helix is drastically different from the preferred conformation of the polymer with methyl side-chains, where the C–Si bonds in the backbone have a slight preference for the t state. The calculated repeat distance along the axis of this helix is 4.90 Å if $l = 1.89$ Å, $\theta = 116°$, and $\phi = 68°$ [23].

Of course, a different structure might be preferred if only one of the two side-chains at each silicon atom is longer than a methyl group. The result might be affected by the use of an oxygen atom, rather than a carbon atom, in the attachment of a side-chain to the silicon atom in the backbone, because the van der Waals radius of an oxygen atom is about 0.6 Å smaller than the van der Waals radius of a methylene group. These issues are addressed in the next section, where the larger side-chain is $-O(CH_2)_NOC_6H_4C_6H_5$.

3. The backbone of poly[Si(CH$_3$)OR–CH$_2$]

We begin by consideration of the bonds in the backbone, in the approximation that the $O(CH_2)_NOC_6H_4C_6H_5$ side-chain is truncated to a single oxygen atom. This severe approximation sets aside temporarily the consideration of the different conformations that are accessible to the flexible spacer in the side-chain. After the analysis of the backbone bonds in this approximation, the modifications required by the introduction of the flexible side-chain will be introduced. The stereochemistry of the attachment of the oxygen atom to a silicon atom will be described using the pseudo d, l notation [28]. A local Cartesian coordinate system is defined for each silicon atom. The x-axis lies along the previous $CH_2{-}Si$ bond, pointing from C to Si. The y-axis is in the plane of $CH_2{-}Si{-}CH_2$, and oriented such that the second CH_2 atom has a positive y coordinate. The z-axis completes a right-handed Cartesian coordinate system. If the oxygen atom bonded to the silicon atom has a positive (or negative) z coordinate, its attachment to Si is defined as d (or l).

In each conformation of a backbone bond, a methylene group in the backbone participates in first-order interactions with two other groups, chosen from the CH_2, CH_3, and O bonded to a silicon atom. The lengths of the Si–C and Si–O bonds, and the differences in the size of O and CH_2 (or CH_3), lead to nearly equivalent energies for the three possible pairs of first-order interactions energies. Therefore the net first-order interactions are equivalent for all stereochemistries of the chains.

For the $Si{-}CH_2{-}Si{-}CH_2{-}Si$ fragment, g states of opposite sign at the bonds to the central silicon atom reduce the separation of the pendant Si to 3.08 Å. This conformation also produces mandatory third order interactions between one of these silicon atoms and the CH_2, CH_3, or O bonded to the other Si atom, which is apparent from Fig. 2, with one of the CH_3 bonded to Si in that figure replaced by an oxygen atom. The separations of the interacting pairs are in the range 1.89–1.99 Å, depending on the choice of CH_2, CH_3, or O. In all cases, the interaction is prohibitively repulsive. The second-order interactions are weak in all of the other states at this pair of bonds. The statistical weight matrix for the $Si{-}CH_2$ bond is therefore independent of the stereochemistry of the chain, and identical with the statistical weight matrix used for this bond by Mark and Ko in their treatment of poly(dimethylsilylenemethylene) [24].

$$\mathbf{U}_{Si-C} = \begin{bmatrix} 1 & 1 & 1 \\ 1 & 1 & 0 \\ 1 & 0 & 1 \end{bmatrix} \qquad (4)$$

A different situation is obtained for the pair of Si–C bonds to the methylene group between two silicon atoms. In every possible state for this pair of bonds, there are two ‘pentane-effect’ second order interactions involving two atoms bonded to one silicon atom interacting with two atoms bonded to the other Si. Four distinct pairs of second-order interactions are possible, as depicted in the four panels of Fig. 3. There are significant differences in the energies of these mandatory pairs of second-order interactions. Conformational energy calculations with the COMPASS force field and Cerius^2 version 4.0 from Accelrys, Inc., find the relative energies to be 0, 1.3, 3.7, and 8.4 kJ/mol, in the same order as the panels of Fig. 3. Let the statistical weights be denoted by 1, ω_a, ω_b, and ω_c, respectively. The pattern of the appearance of these statistical weights in the statistical weight matrix for the C–Si bond depends on the stereochemistry of the attachment of the oxygen atom to the two silicon atoms on either side of the central methylene group.

$$\mathbf{U}_{C-Si,dd} = \mathbf{Q}\mathbf{U}_{C-Si,ll}\mathbf{Q} = \begin{bmatrix} \omega_a & 1 & \omega_b \\ \omega_b & \omega_b & \omega_c \\ 1 & \omega_a & \omega_b \end{bmatrix} \qquad (5)$$

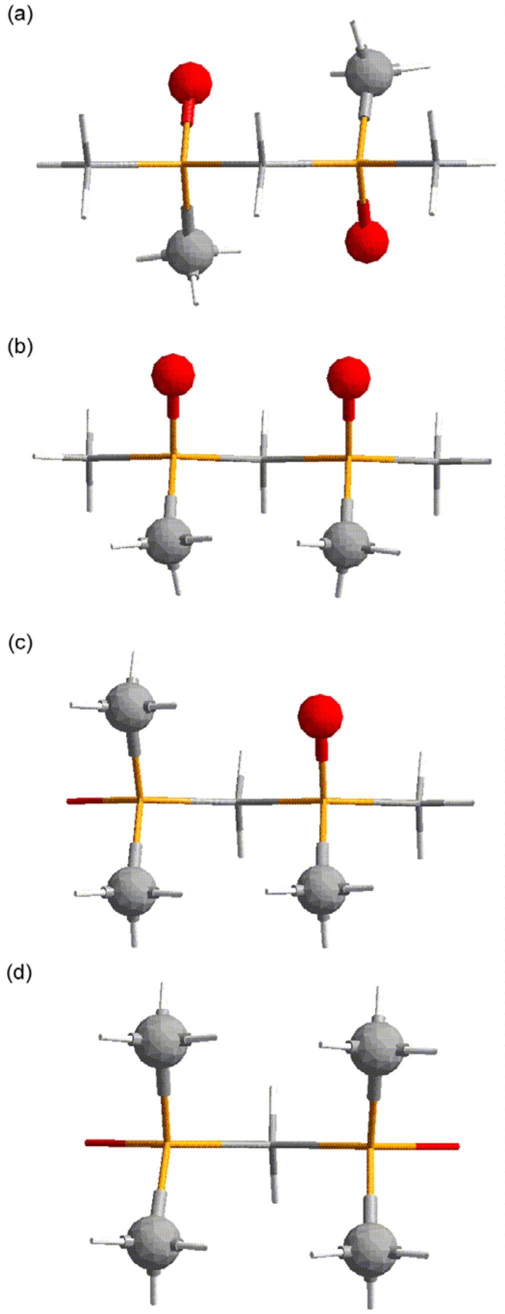

Fig. 3. The pairs of second-order interactions in various conformations of the two bonds to the bridging methylene unit in $-OSi(CH_3)_2-CH_2-Si(CH_3)_2O-$. The four panels are depicted in the order of increasing conformational energy, with the pairs of interacting atoms being (a) C···O and C···O, (b) C···C and O···O, (c) C···C and C···O, and (d) C···C and C···C. The atoms participating in the second-order interactions are drawn as spheres. Sticks represent the C–H bonds to the sphere representing the carbon atom of the methyl group.

$$\mathbf{U}_{\mathrm{C-Si},dl} = \mathbf{Q}\mathbf{U}_{\mathrm{C-Si},ld}\mathbf{Q} = \begin{bmatrix} 1 & \omega_\mathrm{b} & \omega_\mathrm{a} \\ \omega_\mathrm{b} & \omega_\mathrm{c} & \omega_\mathrm{b} \\ \omega_\mathrm{a} & \omega_\mathrm{b} & 1 \end{bmatrix} \tag{6}$$

$$\mathbf{Q} = \begin{bmatrix} 1 & 0 & 0 \\ 0 & 0 & 1 \\ 0 & 1 & 0 \end{bmatrix} \tag{7}$$

In this approximation, the hypothetical isotactic and syndiotactic chains have characteristic ratios of 4.5 and 4.7, respectively. These two values of C are slightly larger than the value of 3.7 calculated for poly(dimethylsilylenemethylene) at the same temperature. The populations of the t state are 0.52 and 0.55 for the isotactic and syndiotactic chain, respectively. They are higher than the value of 0.44 for poly(dimethylsilylenemethylene). More insight into the preferred chain conformations is obtained by examination of the probabilities for the conformations at pairs of bonds, which is denoted by $p_{\xi\eta;i}$ when the second bond is bond i [17]. In matrix form, the $p_{\xi\eta;\mathrm{SiC}}$ and $p_{\xi\eta;\mathrm{CSi}}$ for the *meso* (*dd*) chain are

$$\begin{bmatrix} 0.21 & 0.08 & 0.23 \\ 0.23 & 0.08 & 0 \\ 0.08 & 0 & 0.08 \end{bmatrix} \begin{bmatrix} 0.24 & 0.20 & 0.09 \\ 0.09 & 0.05 & 0.02 \\ 0.20 & 0.07 & 0.05 \end{bmatrix} \tag{8}$$

For the *dl* dyad from the syndiotactic chain, the $p_{\xi\eta;\mathrm{SiC}}$ and $p_{\xi\eta;\mathrm{CSi}}$ are

$$\begin{bmatrix} 0.25 & 0.08 & 0.23 \\ 0.23 & 0.07 & 0 \\ 0.08 & 0 & 0.07 \end{bmatrix} \begin{bmatrix} 0.33 & 0.09 & 0.13 \\ 0.09 & 0.02 & 0.05 \\ 0.13 & 0.05 & 0.12 \end{bmatrix} \tag{9}$$

For each matrix in Eqs. (9) and (10), the stereochemistry is inverted by pre- and postmultiplication by **Q**. When averaged over the entire chain, the combined $p_{\xi\eta}$ for *tt* and the two most stable *tg* helices account for 2/3 of the total probability. The syndiotactic chain has a slightly stronger preference for *tt* ($p_{\xi\eta}$ is 0.29 for *tt*, vs. 0.36 for the sum of the two most probable *tg* helices) than does the isotactic chain ($p_{\xi\eta}$ is 0.23 for *tt*, vs. 0.43 for the sum of the two most probable *tg* helices). This approximate equivalence of the preference for the extended conformation and the *tg* helices in the isotactic and syndiotactic chains suggests that a small perturbation of each monomer unit might be sufficient to tip the balance in one direction or the other.

When compared with PE, all of the silicon-containing polymers considered so far have smaller p_t and C, as shown in Table 2. We turn now to the manner in which the introduction of the complete $-O(CH_2)_NOC_6H_4C_6H_5$ side-chain affects the RIS model for the polymer, in the approximation that first-, second-, and mandatory third-order interactions (but no interactions of higher order) are considered.

4. The flexible side-chain

The shortest side-chain of interest is $-O(CH_2)_NOC_6H_4C_6H_5$ with $N = 3$ [7]. For reasons that will become apparent momentarily, it is convenient to temporarily set aside the statistical weight matrix for the Si–O bond, and consider first the remaining rotatable bonds in the side-chain.

The short-range interaction energies in the statistical weight matrices for these bonds are presented in Table 3. The form of the result for the first bond listed, the O–C bond nearest the backbone, is especially important. A $t \longrightarrow g$ transition at this bond decreases the Si…CH_2 distance from 3.90 to 2.91 Å, and simultaneously produces a mandatory second-order interaction between the methylene group and one of the carbon atoms (in CH_2 or CH_3) bonded to the silicon atom. The distance of the first-order interaction is 4% larger than the comparable distance in poly(trimethylene oxide), where the interaction energy for the first-order interaction is 3.8 kJ/mol [29]. Since the silicon atom is larger than a carbon atom, we expect this repulsive interaction in the silicon containing polymer to be at least as strong as the comparable first-order interaction in poly(trimethylene oxide). The mandatory second-order interaction between the pair of carbon atoms has a distance that is only 1% larger than the comparable distance in PE [22], suggesting that the energies of these two interactions are similar. The sum of the first-order and mandatory second-order interactions is thereby estimated at 12 kJ/mol. There are no other interactions of consequence. When the mandatory second-order interaction is folded into the first-order interaction, the statistical weight matrix consists of three identical rows, signifying that the conformation of that portion of the side-chain extending from the first methylene through the biphenyl is independent of the conformation of the backbone, in the approximation where only first- and second-order interactions are used. This result will be exploited below, when the statistical weight matrices for the flexible side-chains are combined with the statistical weight matrices for the backbone.

Most of the interactions energies in the remaining rows of Table 3 are equated to the analogous interactions in poly(trimethylene oxide) [29]. The only exception occurs in the second-order interactions listed in the second row of the table. These interactions involve a methylene group and the silicon atom to which the side-chain is attached. The value of ω can be approximated as zero because the relevant conformation has mandatory and highly repulsive third order interactions between the methylene and the carbon atoms bonded to the silicon atom. Conformational energy calculations suggest there is also a slight repulsion when the $O{-}CH_2{-}CH_2$ bonds both occupy g states of the same sign. This weak repulsion is assigned an energy of 0.4 kJ/mol.

Table 3
First- and second-order interaction energies (kJ/mol) for the statistical weight matrices for bonds O–C through C–O in the $O(CH_2)_3OC_6H_4C_6H_5$ side-chain, using the general form in Eq. (1)

Bond	E_σ	E_τ	E_ψ	E_ω
$O{-}CH_2$	12	0	0	0
First $CH_2{-}CH_2$	− 1.7	0	0.4	∞
Second $CH_2{-}CH_2$	− 1.7	0	0	1.7
$CH_2{-}O$	3.8	0	0	∞

The serial product of all of the statistical weight matrices specified in Table 3, and the terminal column in which all elements are 1, is a column with three identical elements. If we are concerned with the mean square unperturbed dimensions of the backbone, the actual value assigned to these identical elements is not important.

We now turn to the consideration of the Si–O bond, which was temporarily deferred at the beginning of this section. Rotation about the Si–O bond defines the position of the first methylene group in the side-chain. In the approximation that the methylene and methyl groups bonded to this silicon atom are equivalent, the first-order interactions are identical in all three states of this bond. The second-order interactions involve the first methylene in the side-chain with the silicon atoms on either side of the Si to which the side-chain is bonded. The mandatory third-order interactions in the closest approach of the methylene with one of these silicon atoms requires complete suppression of these conformations. However, the next closest approach of these atoms yields a significant attraction, estimated at − 4.7 kJ/mol upon calculation of the conformational energy surface with the COMPASS force field from Accelrys, Inc. A more strongly negative value is obtained with the Universal 1.02 force field. The less negative value is used in the calculation described, and the consequences of the uncertainty in this attractive energy will be assessed. Let ψ denote the statistical weight for this attractive second-order interaction between the side-chain and the backbone.

Proper incorporation of these second-order interactions into the matrix expression for Z requires a method that takes account of the interaction of the first methylene in the side-chain bonded to silicon atom i with Si atoms bearing indices $i \pm 2$. The methodology was established originally for vinyl polymers with articulated side-chains [30,31]. The method adopted here uses a 3×9 matrix with rows indexed by the state at the $CH_2{-}Si$ bond between chain atoms $i-1$ and i. The order of indexing is t, $g+$, $g-$, with the state defined by chain atoms $i-2$ through $i+1$. The columns are indexed by the states at two other bonds to the silicon atom that bears index i. One bond is the $Si{-}CH_2$ bond to chain atom $i+1$, with the columns indexed in the order $t, t, t, g+, g+, g+, g-, g-, g-$. The matrix will include the first- and second-order interactions for this bond, as well as the Si–O bond. The other bond is, of course, the Si–O bond, with the state defined by chain atoms $i-1$ and i, along with the OCH_2 in the side-chain. For this bond, the columns are indexed in the order $t, g+, g-, t, g+, g-, t, g+, g-$. If the attachment of the side-chain to Si atom i defines a d placement, the matrix is

$$\mathbf{U}_{b;d} = \begin{bmatrix} 0 & \psi^2 & 0 & 1 & \psi & 0 & \psi & 0 & 0 \\ 0 & 0 & \psi & 1 & 0 & \psi & 0 & 0 & 0 \\ 0 & \psi & 1 & 0 & 0 & 0 & \psi & 0 & 1 \end{bmatrix} \qquad (10)$$

The null elements at the last three positions in the second row, and positions 4–6 in the third row, arise from the prohibitively repulsive interaction of silicon atoms $i \pm 2$ when there are g placements of opposite sign at the two C–Si bonds to silicon atom i. The null elements in columns 1 and 8 arise from similar interactions of the CH_2 group in the side-chain with silicon atom $i+2$ and its substituents. The remaining null elements are from similar repulsive interactions between the CH_2 group in the side-chain and silicon atom $i-2$. The ψ-type interactions occur between the CH_2 in the side-chain and the silicon atom at $i+2$ in columns 2 and 7, and between the same CH_2 group and the Si atom at position $i-2$ in elements $1, 2+k$ and elements $2, 3+k$ for $k = 0, 3, 6$. The conformation with a t state at both C–Si bonds and a $g+$ state at the Si–O bond is unique because it is the only combination of states at these three bonds that produces two of the attractive ψ-type interactions. This unique conformation has important consequences for the conformation of the chain. It is depicted in Fig. 4.

If the attachment of the side-chain produces the l configuration, the matrix changes to

$$\mathbf{U}_{b;l} = \mathbf{Q}\mathbf{U}_{b;d}(\mathbf{Q}\otimes\mathbf{Q})$$

$$= \begin{bmatrix} 0 & 0 & \psi^2 & \psi & 0 & 0 & 1 & 0 & \psi \\ 0 & 1 & \psi & \psi & 1 & 0 & 0 & 0 & 0 \\ 0 & \psi & 0 & 0 & 0 & 0 & 1 & \psi & 0 \end{bmatrix} \qquad (11)$$

The unique conformation with two attractive ψ-type interactions still has t states at the two C–Si bond, but there is now a $g-$ state at the Si–O bond.

In the construction of an expression for Z for the backbone of the polymer, the contribution of a dyad constructed from two pseudoasymmetric centers with configuration mm', where m and m' are chosen from d and l, is incorporated into the expression for Z as the 3×3 matrix defined as

$$\mathbf{U}_{b;m}(\mathbf{U}_{\mathrm{C-Si},mm'}\otimes\mathbf{U}_{\mathrm{s}}) \qquad (12)$$

$\mathbf{U}_{b;m}$ is from Eq. (10) or Eq. (11), and $\mathbf{U}_{\mathrm{C-Si},mm'}$ is from Eq. (5) or Eq. (6), and $\mathbf{U}_{\mathrm{s}} = [\,1 \quad 1 \quad 1\,]^{\mathrm{T}}$ [31].

At 373 K, the population of the t state is 0.69 for the isotactic chain and 0.76 for the syndiotactic chain. These values are larger than the estimates for any of the other chains listed in Table 2. Incorporation of the articulated side-chain increases the population of the t state at the C–Si bonds in the backbone. The consequences for the unperturbed dimension are depicted in Fig. 5 for chains with several repeating stereochemical sequences, as a function of the probability of a *meso* dyad, p_{m}. All of the characteristic ratios in Fig. 5 are much larger than the value of 3.7 calculated at the same temperature $[Si(CH_3)_2{-}CH_2]_x$. Replacement of one of the methyl groups with the $-O(CH_2)_NOC_6H_4C_6H_5$ side-chain in each monomer unit increases the mean square unperturbed dimensions by approximately a factor of 2–3, depending on the stereochemical sequence. There is a simple monotonic relationship between C_∞ and p_{m}. The largest dimensions are obtained with the syndiotactic chain.

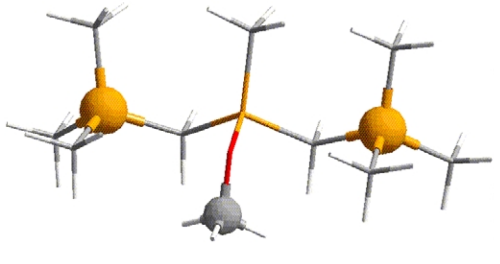

Fig. 4. The conformation of $(CH_3)_3Si{-}CH_2{-}Si(OCH_3)(CH_3){-}CH_2{-}Si(CH_3)_3$ that produces two attractive ψ-type interactions. The atoms involved in these interactions are represented as spheres.

In contrast with poly(dimethylsilylenemethylene), the polymers with the $-O(CH_2)_xOC_6H_4C_6H_5$ side-chain have large, negative temperature coefficients for the unperturbed dimensions, which are about $-3\times 10^{-3}\ \mathrm{K}^{-1}$ for the isotactic chain and $-6\times 10^{-3}\ \mathrm{K}^{-1}$ for the syndiotactic chain.

The explanation for the effect of the side-chain on the unperturbed dimensions can be developed by starting with the probabilities for conformations at neighboring pairs of CH_2–Si bonds in the main chain, using the same format as was adopted in Eqs. (8) and (9). The $p_{\xi\eta}$, in the order Si–CH_2 bond, CH_2–Si bond, are

$$\begin{bmatrix} 0.50 & 0.05 & 0.14 \\ 0.14 & 0.06 & 0 \\ 0.05 & 0 & 0.06 \end{bmatrix}\begin{bmatrix} 0.44 & 0.16 & 0.09 \\ 0.09 & 0.02 & 0.01 \\ 0.16 & 0.02 & 0.02 \end{bmatrix} \qquad (13)$$

for the dd dyad in an isotactic chain and

$$\begin{bmatrix} 0.61 & 0.05 & 0.11 \\ 0.11 & 0.04 & 0 \\ 0.05 & 0 & 0.04 \end{bmatrix}\begin{bmatrix} 0.60 & 0.07 & 0.10 \\ 0.07 & 0.01 & 0.02 \\ 0.10 & 0.02 & 0.03 \end{bmatrix} \qquad (14)$$

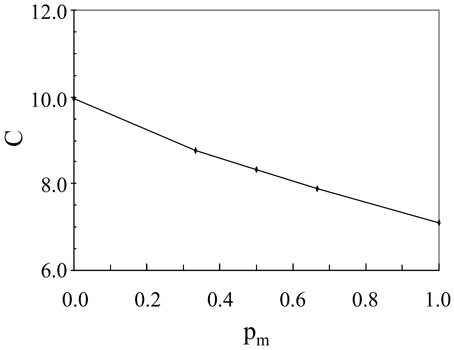

Fig. 5. Characteristic ratios at 373 K for the polymer of $-Si(CH_3)[O(CH_2)_NOC_6H_4C_6H_5]{-}CH_2{-}$ as a function of the probability of a *meso* dyad. The calculation incorporates all first- and second-order interaction, as well as the higher order interactions that are mandatory in some of the local conformations. The results were obtained for polymers with repeating stereochemical sequences of r, mrr, mr, mmr, and m, where m and r denote *meso* and *racemo* dyads, respectively.

for the *dl* dyad in a syndiotactic chain, all calculated at 373 K. The averages of the values of the 1,1 elements in each pair of matrices are the value of p_{tt} for each chain. They are reported in Table 2. The influence of the articulated side-chain is succinctly summarized by comparison of the values for p_{tt} in the last four entries in the Table 2. Inclusion of the entire side-chain doubles the probability that two consecutive C–Si bonds in the backbone will both be in *t* states, and this doubling takes place without regard to the stereochemistry of the dyad. This value of p_{tt} is enhanced by the simultaneous attractive second-order interaction of the first methylene group in the side-chain and the silicon atoms on either side of the Si to which the side-chain is bonded, as depicted in Fig. 4. These two attractive second order interactions can occur in either *meso* or *racemo* dyads, provided there are *t* states at both Si–C bonds to the silicon atom that bears the side-chain.

The similar occurrence of this attractive second-order interaction in both types of dyads causes chains of all stereochemical compositions, including atactic chains of any conceivable stereochemical composition and stereochemical sequence, to have a preferred conformation that consists of runs of *t* states. This preference becomes slightly stronger as the population of *racemo* dyads increases, because that situation existed in the hypothetical polymer in which the side-chain was truncated at the first oxygen atom. As expected from these considerations, the results obtained from the RIS analysis of the substituted poly(silylenemethylenes) are more sensitive to variation in the value assigned to ψ than in the values of any of the ω's, as shown in Table 4. The most critical of the ω's is ω_a for the isotactic chain, and ω_b for the syndiotactic chain.

This preferred conformation approximates one of the two candidates for the smectic E phase described by Park et al. [7], although it is not the *g* helix that was their preferred candidate. They find the *g* helix is favored by interactions between the long side-chains on neighboring silicon atoms that are of longer range than the interactions usually considered in a RIS model. A simulation of a dense system of suitably constrained coarse-grained chains will be required to assess the influence of the intra- and intermolecular interactions of the biphenyl groups on the structure of the system. The intermolecular interactions might alter the preferred conformation of the backbone in the liquid crystalline state [7]. The RIS model described here will constitute one of the constraints on the conformations of the coarse-grained chains in these simulations.

Table 4
Sensitivity of C_∞ and the population of the *t* state to variation in the statistical weights at 373 K

Tacticity	x	$\partial \ln C_\infty/\partial \ln x$	$\partial \ln p_t/\partial \ln x$	$\partial \ln p_{tt}/\partial \ln x$
Isotactic	ψ	0.51	0.22	0.50
	ω_a	0.46	0.20	0.45
	ω_b	−0.19	−0.12	−0.23
	ω_c	−0.05	−0.01	−0.01
Syndiotactic	ψ	0.84	0.25	0.44
	ω_a	−0.23	−0.07	−0.17
	ω_b	−0.45	−0.11	−0.20
	ω_c	−0.01	−0.01	−0.01

The significance of the ψ interaction for the adoption of a regular periodic structure by an atactic chain can be stated more generally. A regular structure for an atactic chain can be anticipated if the same conformation is preferred by both types of *meso* dyads (*dd* and *ll*, in the notation using pseudoasymmetric centers) as well as by both types of *racemo* dyads (*dl* and *ld*). If the bonds in the chain are subject to a three-fold torsion potential with *t*, *g*+, and *g*− states, this condition is most easily satisfied if all of the dyads have short-range interactions that induce a preference for the *t* state at the bonds in the backbone. The ψ interaction described here for the poly(silylenemethylenes) is an example of how this circumstance might be achieved in a real polymer. Of course, Nature might provide other types of short-range interactions that could achieve the same objective in other polymers.

A preference for the *t* state does not necessarily imply that the preferred structure must be a fully extended chain. The adoption of *t* states at every bond does indeed produce a fully extended chain if all bond angles are equal, as they are in PE. But if the bond angles are unequal and alternate in size, $\theta_i = \theta_{i+2} = \ldots \neq \theta_{i+1} = \theta_{i+3} = \ldots$, the all-*t* chain can describe a circle. A well-known example is provided by poly(dimethylsiloxane) [32–34]. Small, and correlated, adjustments of the torsion angle for the *t* state, from $\phi = 180°$ to $\phi = 180° + \Delta\phi$, will convert the planar circular conformation of the all-*t* chain to a helix. By this route, an atactic chain with *t* states at every bond could form a helix with a pitch just large enough so that successive turns of the helix would not interact with one another in a repulsive manner, as they obviously would do if every torsion angle was precisely 180°.

5. Conclusion

A RIS analysis incorporating first- and second-order interactions, as well as those third-order interactions that are mandatory in several of the conformations, shows that poly(silylenemethylenes) with $-O(CH_2)_NOC_6H_4C_6H_5$ side-chains have the same preferred conformation of the backbone, independent of the stereochemical sequence. This preferred conformation is a sequence of *t* states at the C–Si bonds. It is favored by an attractive second-order interaction between the first methylene group in the $-O(CH_2)_NOC_6H_4C_6H_5$ side-chain at position *j* and the two silicon atoms with indices $j \pm 2$. This interaction is independent of the stereochemistry of the attachment of the side-chain to silicon atom *j*. Therefore atactic chains have the same preferred conformation of the backbone as do isotactic and syndiotactic chains, which may facilitate the formation of liquid crystalline structures by chains with an atactic backbone.

The first- and second-order interactions at the first O–C bond in the side-chain impose a strong preference for the *t* state at this bond, which tends to extend the side-chain away from the backbone. These interactions also cause the conformation of the flexible spacer in the side-chain to be independent of the conformation of the backbone, in the approximation where only first- and second-order interactions are considered. Interactions of much higher order between the side-chains may also affect the conformations of the chains. The potential influence of these higher order interactions is more easily assessed by another method, such as Monte Carlo simulation.

Acknowledgements

This research was supported by the Collaborative Center in Polymer Photonics, funded by the Air Force Office of Scientific Research, Wright–Patterson Airforce Base, and the University of Akron. D.C. thanks Malone College for granting him the sabbatical leave for his contribution to this article.

References

[1] Nagai K. Molecular configuration of vinyl polymers with strictly regular structures and their mean dimensions and electric moments in dilute solution. J Chem Phys 1959;30:660.

[2] Natta G, Corradini P, Ganis P. Chain conformation of polypropylene having regular structure. Makromol Chem 1960;39:238.

[3] Flory PJ, Mark JE, Abe A. Random-coil configuration of vinyl polymer chains. The influence of stereoregularity on the average dimensions. J Am Chem Soc 1966;88:639.

[4] Ishihara N, Seimiya T, Kuramoto M, Uoi M. Crystalline syndiotactic polystyrene. Macromolecules 1986;19:2464.

[5] Chatani Y, Maruyama H, Noguchi K, Asanuma T, Shiomura T. Crystal structure of the planar zigzag form of syndiotactic polypropylene. J Polym Sci, Part C: Polym Lett 1990;28:393.

[6] Percec V, Ah CH, Cho WD, Jamieson AM, Kim J, Leman T, Schmidt M, Gerle M, Möller M, Prokhorova SA, Sheiko SS, Cheng SZD, Zhang A, Ungar G, Yeardley DJP. Visualizable cylindrical macromolecules with controlled stiffness from backbones containing libraries of self-assembling dendritic side groups. J Am Chem Soc 1998;120:8619.

[7] Park SY, Zhang T, Interrante LV, Farmer BL. Structures of side-chain liquid crystalline poly(silylenemethylene)s. Macromolecules 2002; 35:2776.

[8] Baschnagel J, Binder K, Doruker P, Gusev AA, Hahn O, Kremer K, Mattice WL, Müller-Plathe F, Murat M, Paul W, Santos S, Suter UW, Tries V. Bridging the gap between atomistic and coarse-grained models: status and perspectives. Adv Polym Sci 2000;152:41.

[9] Doruker P, Mattice WL. Reverse mapping of coarse grained polyethylene chains from the second nearest neighbor diamond lattice to an atomistic model in continuous space. Macromolecules 1997;30:5520.

[10] Clancy TC, Pütz M, Weinhold JD, Curro JG, Mattice WL. Mixing of isotactic and syndiotactic polypropylenes in the melt. Macromolecules 2000;33:9452.

[11] Lohse DJ. The melt compatibility of blends of polypropylene and ethylene–propylene copolymers. Polym Engng Sci 1986;26:1500.

[12] Maier RD, Thomann R, Kressler J, Mülhaupt R, Rudolf G. The influence of stereoregularity on the miscibility of polypropylene. J Polym Sci, Part B 1997;35:1135.

[13] Thomann R, Kressler J, Setz S, Wang C, Mülhaupt R. Morphology and phase behavior of blends of syndiotactic and isotactic polypropylene. 1. X-ray scattering, light microscopy, atomic force microscopy, and scanning electron microscopy. Polymer 1996;37: 2627.

[14] Thomann R, Kressler J, Rudolf B, Mülhaupt R. Morphology and phase behavior of blends of syndiotactic and isotactic polypropylene. 2. Differential scanning calorimetry, light transmission measurements, and PVT measurements. Polymer 1996;37:2635.

[15] Clancy TC, Mattice WL. Role of the attractive portion of the Lennard–Jones potential in the homogeneity of melts of isotactic and syndiotactic polypropylene. J Chem Phys 2001;115:8221.

[16] Xu G, Clancy TC, Mattice WL, Kumar SK. Increase in the chemical potential of syndiotactic polypropylene upon mixing with atactic or isotactic polypropylene in the melt. Macromolecules 2002;35:3309.

[17] Flory PJ. Foundation of rotational isomeric state theory and general method for generating configuration averages. Macromolecules 1974; 7:381.

[18] Rapold RF, Mattice WL. Introduction of short and long range energies to the simulation of real chains on the 2nd lattice. Macromolecules 1996;29:2457.

[19] Haliloglu T, Mattice WL. Mapping of rotational isomeric state chains with asymmetric torsional potential energy functions on a high coordination lattice: application to polypropylene. J Chem Phys 1998; 108:6989.

[20] Cho J, Mattice WL. Estimation of long range interaction in coarse-grained rotational isomeric state polyethylene chains on a high coordination lattice. Macromolecules 1997;30:637.

[21] Clancy TC, Jang JH, Dhinojwala A, Mattice WL. Orientation of phenyl rings and methylene bisectors at the free surface of atactic polystyrene. J Phys Chem B 2001;105:11483.

[22] Abe A, Jernigan RL, Flory PJ. Conformational energies of *n*-alkanes and the random configuration of high homologs including polymethylene. J Am Chem Soc 1966;88:631.

[23] Park SY, Interrante LV, Farmer BL. The structure of poly(di-*n*-propylsilylenemethylene). Polymer 2001;42:4253.

[24] Mark JE, Ko JH. Configuration-dependent properties of poly(dimethylsilmethylene) chains. II. correlation of theory and experiment. Macromolecules 1975;8:874.

[25] Tsao MW, Pfeifer KH, Rabolt JF, Holt DB, Farmer BL, Interrante LV, Shen Q. Studies of the solid-state conformation of polysilmethylene: An organic/inorganic hybrid polymer with an alternate C/Si backbone. Macromolecules 1996;29:7130.

[26] Sundararajan PR. Conformational aspects of poly(dimethylsilaethylene), an analog of polyisobutylene. Comput Polym Sci 1991;1: 18.

[27] Ko JH, Mark JE. Configuration-dependent properties of poly(dimethylsilmethylene) chains. I. Experimental results. Macromolecules 1975;8:869.

[28] Mattice WL, Suter UW. Conformational theory of large molecules. New York: Wiley; 1994. p. 175.

[29] Abe A, Mark JE. Conformational energies and the random coil dimensions and dipole moment of the polyoxides $CH_3O[(CH_2)_yO]_xCH_3$. J Am Chem Soc 1976;98:6468–76.

[30] Abe A. Optical rotatory properties of vinyl polymers. J Am Chem Soc 1968;90:2205.

[31] Mattice WL. Configuration partition functions for vinyl polymers containing articulated side-chains with threefold rotational potentials. Macromolecules 1977;10:1171.

[32] Flory PJ, Crescenzi V, Mark JE. Configuration of the poly(dimethylsiloxane) chain. III. Correlation of theory and experiment. J Am Chem Soc 1964;86:146.

[33] Beevers MS, Semlyen JA. Equilibrium ring concentrations and the statistical conformation of polymer chains. 8. Calculation of small ring concentrations in poly(dihydrogensiloxane) and poly(dimethylsiloxane) equilibrates. Polymer 1972;13:385.

[34] DeBolt LC, Mark JE. Models for the trapping of cyclic poly(dimethylsiloxane) (PDMS) chains in PDMS networks. Macromolecules 1987;20:2369.